Environmental Science & Technology

pubs.acs.org/est

Article

Anaerobic Dehalogenation by Reduced Aqueous Biochars

Srinidhi Lokesh, Juhee Kim, Yuwei Zhou, Danping Wu, Bo Pan, Xilong Wang, Sebastian Behrens, Ching-Hua Huang, and Yu Yang*

Cite This: *Environ. Sci. Technol.* 2020, 54, 15142−15150

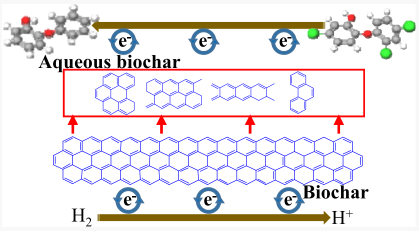

ABSTRACT: Dehalogenation is one of the most important reactions for eliminating trace organic pollutants in natural and engineering systems. This study investigated the dehalogenation of a model organohalogen compound, triclosan (TCS), by aqueous biochars (a-BCs) (<450 nm). We found that TCS can be anaerobically degraded by reduced a-BCs with a pseudo first-order degradation rate constant of 0.0011−0.011 h^{-1}. The 288 h degradation fraction of TCS correlated significantly with the amount of a-BC-bound electrons (0.055 ± 0.00024 to 0.11 ± 0.0016 mol e^-/mol C) available for donation after 24 h of pre-reduction by *Shewanella putrefaciens* CN32. Within the reduction period, the recovery of chlorine based on residual TCS and generated Cl^- ranged from 73.6 to 85.2%, implying that a major fraction of TCS was fully dechlorinated, together with mass spectroscopic analysis of possible degradation byproducts. Least-squares numerical fitting, accounting for the reactions of hydroquinones/semiquinones in a-BCs with TCS and byproducts, can simulate the reaction kinetics well ($R^2 > 0.76$) and suggest the first-step dechlorination as the rate-limiting step among the possible pathways. These results showcased that the reduced a-BCs can reductively degrade organohalogens with potential applications for wastewater treatment and groundwater remediation. While TCS was used as a model compound in this study, a-BC-based degradation can be likely applied to a range of redox-sensitive trace organic compounds.

INTRODUCTION

Organohalogen compounds, utilized in a variety of industrial applications, cause persistent harmful effects to ecosystems and human health.[1−5] Their widespread use in solvents, degreasing agents, biocides, and many other products requires large volumes to be synthesized.[6−8] Once used, organohalogen compounds are ultimately released into the environment, raising concerns about the toxicity of these compounds and their environmental effects.[9−13]

Most organohalogen compounds are persistent and hard to degrade; with half-lives of up to 34 years, they pose challenges for engineering treatment and remediation.[14−22] Dehalogenation is the most critical step in the degradation of organohalogen compounds. Uncovering effective dehalogenation reactions and developing efficient engineering treatment processes for the degradation of organohalogens are needed for wastewater treatment as well as remediation of polluted soils and groundwater.[8,23−27]

As a potential cost-effective material to be used for environmental treatment and remediation, biochars have attracted considerable interest for their application in environmental engineering systems.[28−31] The chemical properties of biochars can enable them to potentially reductively degrade organic compounds, including organohalogens.[32−35] A few recent studies have shown that bulk biochar particles can promote the dehalogenation of organohalogens, e.g., tetrabromobisphenol A and pentachlorophenol, by mediating the electron transfer.[36,37] However, sorption by bulk biochar particles may reduce the bioavailability of the compounds and inhibit their susceptibility to biodegradation, and sorbed organohalogens can cause long-term concerns due to their persistence.[38−41] Instead, if bulk biochars are mobilized to the aqueous phase ("a-BCs"), a-BCs potentially could mainly accelerate the degradation of organohalogens but not affect their bioavailability. In addition, the reactions between a-BCs and organohalogens can be controlled by the degree of reduction of a-BCs. The fully reduced a-BCs may degrade organohalogens more rapidly or thoroughly as more electrons are available for donation to the organohalogens. Up to date, although more and more interest has been given to characterizations and applications of biochars in the aqueous phase, such as those nano-sized,[42,43] no reported studies have comprehensively examined the reactions between a-BCs and organohalogens and unambiguously determined the critical processes.

Herein, this study aimed to investigate the reaction between reduced a-BC and organohalogens using triclosan (TCS) as a model compound. TCS is among the most common contaminants in surface waters and wastewaters in the United States due to its widespread usage and remains a problem for water quality in many regions even after the ban on its primary

Received: September 2, 2020
Revised: October 8, 2020
Accepted: October 29, 2020
Published: November 10, 2020

ACS Publications

https://dx.doi.org/10.1021/acs.est.0c05940

usage.[44,45] There are three chlorine atoms in one TCS molecule, which makes TCS a suitable model compound for studies regarding the dehalogenation process. The primary objectives of this study were to (1) investigate the reactions of TCS with various types of a-BC generated from different parent materials, including bulk-activated carbon (AC) as a reference for comparison, (2) study the controlling factors for the degradation of TCS by a-BC, including the available electrons for donation, and (3) analyze the byproducts and pathways for the degradation of TCS by a-BC.

METHODS AND MATERIALS

Materials. Triclosan (≥98% purity) was purchased from Sigma-Aldrich (St. Louis, MO, U.S.A.). The stock solution of 100 mg/L TCS was made in methanol (≥99.9%, Sigma-Aldrich). Bulk corn biochar was produced by pyrolysis of corn straw at 200 °C (CBC200) and 400 °C (CBC400). Bulk Swiss biochar (SW) was bought from Swiss Biochar Sárl, Switzerland. Slashed materials from pinyon pine-juniper wood were pyrolyzed in steel kilns to prepare the UBCX biochars.[46] The biochar prepared was then sieved through US sieves #28 (600 μm), #35 (425 μm), #48 (300 μm), and #100 (150 μm). The fractions retained by sieve #28 (>600 μm) and #100 (150–300 μm) were used for the experiments and named as UBCL and UBCS, respectively.[47] Granular activated carbon (FILTRASORB 400) was purchased from Calgon Carbon (Moon Township, PA, USA) (Supporting Information, Table S1). All the other chemicals used in this study were of analytical grade. The strain *Shewanella putrefaciens* (*S. putrefaciens*) CN32 was kindly donated by Dr. Scott Fendorf of Stanford University.

Preparation and Characterization of a-BCs. To make the working solutions of a-BCs, bulk biochars (BCs) were suspended in MilliQ water (18.3 MΩ·cm) with a ratio of 100 mg BC:10 mL MilliQ water. The mixture was shaken horizontally at 150 rpm for seven days. Then, the mixture was filtered through a 0.45 μm glass fiber filter to get a-BCs (<450 nm). The total organic carbon contents in the a-BCs were measured with a Shimadzu TOC-VCSH (Kyoto, KYT, Japan). Size fraction analysis of a-BCs was carried out by centrifuging samples at 3000 g for 15 min with an Amicon centrifugal filter unit (cutoff molecular size of 3 kDa) (Sigma-Aldrich, St. Louis, MO), and the total organic carbon content in fractions smaller than 3 KDa was measured. For investigating the chemical compositions and their roles in the degradation of TCS, partial biochar samples were analyzed with a fusion Orbitrap mass spectrometer (MS) (Thermo Fisher Scientific, U.S.A.). More detailed information about MS analysis can be found in the Supporting Information.

Microbial Reduction of a-BC and Electron Transfer. Aqueous BC was reduced by *S. putrefaciens* CN32 (10^8 cells/mL), dissimilatory metal-reducing bacteria that can reduce a range of natural organic carbon and biochars, at pH 7 (3 mM bicarbonate buffer) with H_2 in the headspace as the terminal electron donor, and electron transfer to a-BC was monitored by the following reactions between reduced a-BC and Fe(III)-NTA.[48,49] Similar to our recent work, the strain CN32 was grown for 24 h under aerobic conditions in 25 g/L Luria Bertani (LB) soy broth. Then, cells were harvested by centrifugation (4500 g, 20 min at 4 °C) and washed twice with a 3 mM $NaHCO_3$ buffer (pH 7). The washed cells were re-suspended in an O_2-free $NaHCO_3$ buffer (pH 7) and then reacted with a-BC. After different periods of reduction (up to 72 h), the strain CN32 cells were removed by filtration with 0.2 μm sterilized membranes. The filtrate (1 mL) was reacted with 0.1 mL of 10 mM Fe(III)-nitriloacetate (NTA) for 1 min. The resulting Fe(II) was measured as an indicator for the electrons accepted by a-BC using the ferrozine assay following previous studies.[49] In brief, buffered ferrozine (0.1 mL) was added to the sample solution (1 mL) for the measurement of Fe(II)-ferrozine with absorbance at 562 nm. The number of electrons accepted by a-BC was calculated based on the Fe(II) concentration. All the experiments were conducted in triplicate.

Degradation of TCS by Reduced a-BCs. For the investigation of TCS degradation, a-BCs in 3 mM $NaHCO_3$ buffer (pH 7) were pre-reduced by strain CN32 for 24 h, as described above. The concentrations of a-BCs used were determined to be 284.6, 27.3, 9.5, 6.9, 2.8, and 1.2 mg C/L for CBC200, CBC400, UBCS, UBCL, SW a-BC, and aqueous AC, respectively (Table S1). After the reduction, the samples were filtered with 0.2 μm membrane filters to sterilize the reduced aqueous biochars. The filtered samples were then spiked with 1 mg/L TCS. The filtration with 0.2 um filters reduced the concentration of aqueous biochars only moderately (by 16%) for CBC200, which is determined to be minimally reactive and not the focus for most of reaction analysis, and minimally for other samples (<6%). Samples of pre-reduced a-BC spiked with TCS were enclosed in glass vials with thick butyl rubber septa with a headspace of mixed H_2/N_2 (3.5%/96.5%) in an anaerobic glove chamber (COY, Grass Lake, MI) and then incubated in the dark on a rotary shaker (150 rpm) at 25 °C. After different reaction intervals within 288 h, triplicate samples were sacrificed for the analysis of TCS. Three different controls were used (Table S2). (1) aerobic control: TCS was reacted with unreduced a-BC under aerobic conditions with ambient air in the headspace during the reaction; (2) anaerobic control: TCS was incubated with unreduced a-BC under the same anaerobic conditions as in the experiment; and (3) bacteria control: TCS was incubated with only the filtrate of the bacterial cell solution used to reduce a-BC under the same anaerobic protocol as in the experiment. Additional experiments were also conducted to examine the impact of the a-BC concentration (as half and one-third of the original working solution of a-BCs) on the degradation of TCS. For the most reactive a-BC samples (CBC400 and SW), the impact of different pre-reduction periods were analyzed by reacting a-BCs pre-reduced in different periods (6 and 12 h) with TCS.

Analysis of TCS. For the analysis of TCS, the samples were passed through 0.2 μm glass fiber filters. Filtered samples were analyzed using high-performance liquid chromatography (HPLC, Agilent Technologies 1260, Folsom, CA, U.S.A.) equipped with a C18 column (5 μm, 4.6 × 150 mm). TCS was analyzed by detecting the UV absorbance at 284 nm. The mobile phase was 78:22 (v/v) of methanol and MilliQ water with a flow rate of 1 mL/min. The standard curve was established for TCS with concentrations ranging from 100 to 1000 μg/L (Figure S1).

Analysis of Cl^-. To determine the quantity of Cl^- generated during the degradation of TCS, Cl^- was measured using the mercuric thiocyanate method (EPA Method 8113) with a DR 6000 laboratory spectrophotometer.[50,51] Samples (10 mL) were mixed with mercuric thiocyanate solution (0.8 mL) and Fe(III) solution (0.4 mL) and remained static for 2 min after vigorous mixing. The generated orange ferric thiocyanate complex, an index for the amount of Cl^-, was measured by analysis of UV absorption at 455 nm with a detection limit of 0.045 mg/L.

Byproduct Analysis. Standard compounds of 5-chloro-2-(4-chlorophenoxy)phenol (CCPP) (with one-chlorine removal from TCS) and 5-chloro-2-(phenoxy)phenol (CPP) (with two-chlorine removal from TCS) were donated by Dr. Kristopher McNeill and Dr. Jennifer Apell of the Swiss Federal Institute of Technology. The sample was collected during the sacrifice of samples for the identification of TCS at various time points of analysis and was used for LC/MS analysis. The samples were analyzed by an Agilent 1260 Infinity HPLC with a 6230 accurate mass time-of-flight mass spectrometry (LC-TOFMS) system equipped with a Poroshell 120 EC−C18 column (2.1 × 150 mm, 2.7 μm) at 10 μL of the injection volume. The eluent consisted of two mobile phases at a flow rate of 0.4 mL/min with gradient elution: (A) 5 mM ammonium acetate and (B) acetonitrile. The gradient was as follows: B was started at 50% for the first minute, increasing to 55% in 4 min, increasing to 100% in 10 min, and decreasing to 50% in 11 min. Negative electrospray ionization (ESI) at fragmentation voltages of 140, 180, 220, and 250 V with a mass scan range of 50−1000 m/z was conducted. The drying gas was controlled at 9 mL/min at 200 °C. The nebulizer pressure was set at 40 psi, and the capillary was maintained at 4000 V. Data acquisition and data processing were conducted with mass accuracy (exact mass ± 10 ppm), retention time ($t_R \pm 0.5$ min), isotope patterns (deviation of <5%), and formula finding.

Numerical Fitting and Statistical Analysis. IBM SPSS Statistics (version 26, IBM Corp., Armonk, NY, U.S.A.) was used for performing statistical analyses using the Student's t-test, Pearson test, or Spearman test in which $p > 0.1$ was considered insignificant. Model fitting was done with MATLAB 2019 (The Math Works, Inc.). To fit the kinetics for the presumed reactions involved in the degradation of TCS, the toolbox of "fcn2optimexpr" was used for the least-squares fitting.

■ RESULTS AND DISCUSSION

Physicochemical Properties of Bulk and Aqueous Biochars. Bulk biochars with a carbon content of 47.8−73.2% (Table S1), used in this study, represent different types of parent materials, including hardwood like pinewood or pinyon pine-juniper wood and soft biomass material (corn stalk). We also compared corn stalk-derived biochars generated at two different temperatures (200 and 400 °C). Pinyon pine-juniper wood-derived biochars with two different particle sizes (>600 μm and 150−300 μm) were also used to explore the impact of bulk biochar particle size on the release of a-BC and its reactivity. Bulk activated carbon produced through thermal activation has been used as a comparison. The release of a-BC accounted for 0.01−2.85% of bulk biochar-bound C with values highest for CBC200 and lowest for AC; it is higher for the bulk biochars generated with a lower temperature than with a higher temperature (CBC200 > CBC400) and higher for the bulk biochars derived from soft biological materials (corn stalk) than from hardwood.[52,53] The difference between biochars with different particle sizes in the release of a-BC was moderate. Stock suspensions of a-BC contained 284.6, 27.3, 9.5, 6.9, 2.8, and 1.2 mg C/L for a-CBC200, a-CBC400, a-UBCS, a-UBCL, and a-SW, respectively. Size fraction analysis of the a-BCs showed that 20.6%, 53.8%, 61.4%, 56.4%, and 86.9% of a-BC-bound carbon was below 3 KDa as freely dissolved small compounds for CBC200, CBC400, UBCS, UBCL, and SW a-BCs, respectively.

Electron Transfer for a-BC. Electrons accepted by a-BCs during the microbial reduction sharply increased within the first 6−12 h of the reaction and achieved the highest level within 24 h (Figure 1). Electrons accepted by CBC200 a-BC were not detected as well as below 0.0018 mol e^-/mol C based on the experimental detection limit. For other a-BCs at 24 h, the electrons accepted by a-BCs were determined to be 0.11, 0.047, 0.020, 0.011, and 0.0054 mol e^-/mol C for aqueous biochar of AC, SW, UBCL, UBCS, and CBC400, respectively. The amount of electrons accepted per molar carbon was, in general, higher than that measured for bulk biochars, as high as approximately 0.012 mol e^-/mol C, indicating the favorable leaching for the components enriched in electron-accepting domains, presumably quinoid groups.[35,54,55] SW and UBCL a-BCs had relatively higher electron acceptance capacity, indicating the higher density of electron-accepting moieties. The electron accepting capacity was higher for hardwood-derived a-BCs, e.g., SW, UBCL, and UBCS a-BCs, than that from the soft biomass material of corn stalk, consistent with previous results.[56,57] For corn-derived a-BC, the electron acceptance capacity was higher for samples generated at a higher temperature (400 °C) than that of those produced at 200 °C. It could be due to the higher formation of hydroxyl groups and aromatic structures, including quinoid groups, during the pyrolysis at higher temperatures.[35,58,59]

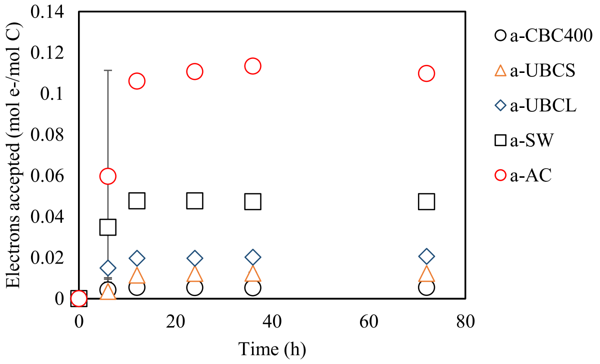

Figure 1. Time-dependent concentrations of electrons accepted by aqueous biochars (a-BCs) during its reduction by *S. putrefaciens* CN32, measured through the consequent reaction with ferric nitrilotriacetate (Fe(III)-NTA). Error bars represent standard deviations obtained from the triplicate experiment with most of them unobservable due to the small size. a-CBC400 denotes aqueous biochar solutions prepared using CBC400 manufactured at 400 °C using corn straw. a-UCBS and a-UCBL denote aqueous biochar solutions prepared using UCBS and b-UBCL manufactured at 500−700 °C using pinyon pine juniper wood. a-SW denotes the aqueous biochar solution prepared using the Swiss biochars manufactured at 700 °C using pine wood, and a-AC denotes the aqueous activated carbon solution prepared using AC manufactured by thermal activation.

For bulk AC, Van der Zee et al.[60] determined the electron acceptance amount of bulk AC with acetate as the terminal electron donor was approximately 0.004 mol e^-/mol C, much lower than the value we determined for the a-AC released. As the reduction potential (E_h^0 vs standard hydrogen electrode) for Fe(III)-NTA/Fe(II) was −587 mV,[61] comparable to the reduction potential of most organohalogens of −500 to 1000 mV (−500 mV for TCS/dechlorinated products),[62−65] the electrons available for donation measured by reduction of Fe(III)-NTA would be relevant for the reaction with organohalogens, such as the model compound TCS in this study.

Kinetics of Triclosan Degradation. Triclosan was degraded anaerobically by the pre-reduced a-BCs with the 288 h degradation fraction ranging from 26.9 ± 1.8% to 93.0 ± 0.6% (Figure 2). As the electron transfer experiment documented that the a-BC-bound donatable electrons achieved the highest value within 24 h, the 24 h-reduced a-BCs were used in this experiment. For the anaerobic control with unreduced a-BCs, the 288 h degradation fraction of TCS was 1.65 ± 1.09% (a-AC) to 27.0 ± 8.58% (a-CBC400). For CBC400 a-BC, the moderate degradation of TCS may indicate the reduction of TCS by the persistent semiquinone groups. When ambient air was used in the headspace for aerobic control, TCS degradation was much less than anaerobic samples with the 288 h degradation fraction of 7.58 ± 1.18% to 18.9 ± 0.71% when O_2 served as a much stronger electron acceptor. The microbial control with the bacteria filtrate under the anaerobic conditions showed less than 20% of TCS to be degraded by the microbial-derived compounds (e.g., extracellular polymeric substances) in the filtrate within 288 h. Chan et al.[66] showed that the reduction potential E^0_H of the EPS released by *Desulfovibrionaceae* and *Desulfobacteriaceae* was −540 mV (standard hydrogen electrode), which was potentially able to degrade TCS reductively.

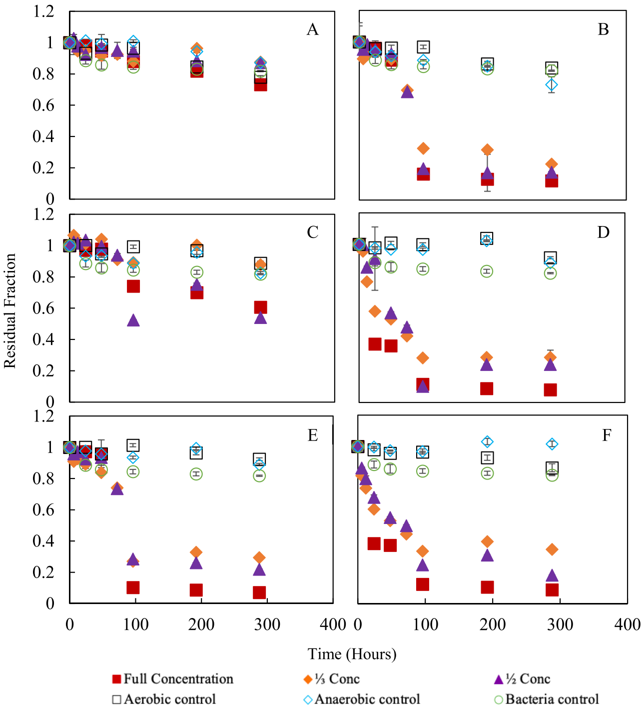

Figure 2. Degradation kinetics of triclosan (TCS) in the presence of different reduced a-BCs: CBC200 (A), CBC400 (B), UBCL (C), UBCS (D), SW (E) a-BC, and aqueous AC (F) at different starting carbon concentrations. Aerobic control, anaerobic control, and bacteria control were also shown. Full concentration indicates samples started directly with a-BC prepared through the leaching of bulk BC with 284.6, 27.3, 9.5, 6.9, 2.8, and 1.2 mg C/L for CBC200, CBC400, UBCS, UBCL, SW a-BC, and aqueous AC. Samples with diluted a-BC (1/2 of the original concentration and 1/3 of the original concentration) were also presented. Error bars indicate the standard error obtained from triplicate experiments with most of them smaller than the symbol.

Compared to controls, the degradation of TCS by the reduced a-BCs under the anaerobic condition was substantially higher, documenting the strong anaerobic reactions between reduced a-BCs and TCS. The 288 h anaerobic degradation fraction of TCS was 26.9 ± 1.80%, 87.8 ± 0.4%, 39.4 ± 0.4%, 92.0 ± 0.2%, 93.0 ± 0.6%, and 91.2 ± 0.2% for reduced CBC200, CBC400, UBCS, UBCL, SW, and AC a-BC, respectively. Degradation of TCS by CBC200 a-BC was lowest with 26.9 ± 1.80% within 288 h, very close to controls (12.9−22.1%). Therefore, the following discussion regarding the reaction kinetics is focused on other biochars except for CBC200 a-BC. Based on the pseudo first-order fittings (r^2 = 0.75−0.99, $p < 0.05$), the rate constant for TCS degradation ranged from 0.00108 h^{-1} to 0.0105 h^{-1}, corresponding to a half-life of 65.8−644 h. Anaerobic degradation of TCS by CBC400 and SW a-BC was relatively slow within the first 24 h. Then, substantial degradation occurred after 24 h, making the kinetics deviate from an apparent first-order kinetic pattern. Such derivation from the first-order pattern indicates more complicated reactions, to be discussed in the sections below. In addition, this study measured the degradation of the total TCS in the solution phase (freely dissolved TCS and TCS associated with a-BC) as the presence of a-BC did not affect the measurement of TCS (Figure S1); the effects of association with a-BC on the availability and reactivity of TCS are expected to be minor and beyond the scope of this work.

The reaction was relatively slower than the abiotic reductive or oxidative reaction of organohalogen with metals. Rate constants for the dehalogenation of polybrominated diphenyl ethers (PBDE) and polychlorinated biphenyl (PCBs) by nano zero-valent iron (nZVI) ranged from 0.0001 to 0.1 h^{-1}.[67,68] Bokare et al.[67] determined that the rate constant for the reaction between TCS and nZVI was around 0.04 h^{-1}, which could be further accelerated by doping of palladium. Trainer et al.[69] found that rate constants for the oxidation of phenol compounds by manganese oxide (δ-MnO_2) ranged from 0.001 to 149 h^{-1} with a value of 7.6 h^{-1} for TCS. The relatively lower reaction rate constants for TCS in this study are primarily because the concentration of a-BC and associated electrons were much lower than the metals. If normalized by the electrons bound with the nZVI, the rate constant for the dehalogenation of PCBs and PBDEs was approximately or below 1 h^{-1}/(mol e^-/L), while the corresponding values in this study ranged from 110 to 560 h^{-1}/(mol e^-/L). This indicates the efficient electron transfer between TCS and a-BC. There are limited studies regarding the microbial dehalogenation mediated by biochar for which the half-lives were similar to this study with a value above 120 h for pentachlorophenol and approximately 480 h for tetrabromobisphenol A.[36,37] A few studies investigated the carbonaceous nanomaterial-mediated reductive dehalogenation.[70,71] Fu et al.[70] showed that the rate constant for reductive degradation of hexachloroethane by sulfide increased from 0.001 to 0.002−0.0045 h^{-1} in the presence of 10 mg/L carbon nanotube or graphene oxide. Although difficult to directly compare, the increase in the rate constant was of the same order of magnitude as the degradation rate constant for TCS in the presence of aqueous biochar used in this study. Such comparison placed the reactions of TCS with a-BC in a potential abiotic method to degrade organohalogens. In addition, the reactions of a-BC have an advantage of having low costs ($2.48/kg for biochar

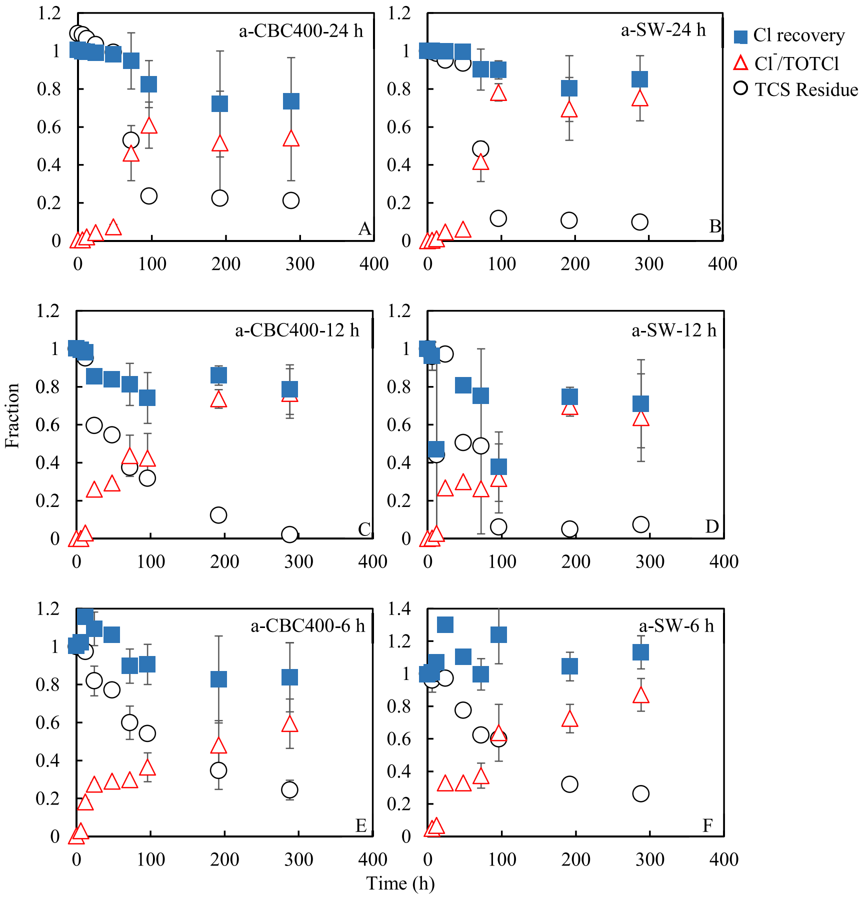

Figure 3. Kinetics for the generation of Cl^- together with the total chlorine recovery and the residual fraction of TCS. Results for the TCS reacted with a-CBC400 and a-SW, pre-reduced for 24, 12, and 6 h, are shown. Error bars represent results from triplicate experiments. a-CBC400 and a-SW represent the aqueous biochar samples prepared using CBC400 and SW, respectively.

compared to \$69/kg for nZVI) and no byproducts in particle phase, compared to the reactions with nZVI.[72,73] These results and analyses indicate significant potential for the application of a-BC in engineering treatment of wastewater and remediation of groundwater.

To evaluate the effects of the amount of a-BC on TCS degradation, TCS was also reacted with different concentrations of a-BC (Figure 2). When the a-BC concentration was decreased, the reactions were slowed down differently. CBC200 a-BC with reduced concentrations showed no significant differences compared to controls (t-test, $p > 0.1$); for UBCS with a concentration of one-third of the stock suspension, the TCS kinetics was also similar to the controls. For other biochars, when the a-BC concentration was reduced to 50% and 33% of the concentration in stock suspensions, the degradation slowed down and the 288 h degradation fraction decreased. When TCS was reacted with CBC400 a-BC of 13.8 mg C/L (1/2 concentration) and 9.2 mg C/L (1/3 concentration), the 288 h degradation fraction was 82.4% and 77.2%, respectively, compared to the value of 87.8% of the reaction with CBC400 a-BC of 27.58 mg C/L. Based on the kinetics, degradation of over 85% of TCS (at an initial concentration of 1.0 mg/L) within the reaction period of 288 h required CBC400, UBCL, SW a-BC, and a-AC at a concentration of 27.6, 7.32, 2.83, and 1.16 mg C/L, respectively.

Bearing analysis uncertainty, the fitted pseudo first-order reaction rate constants were correlated with the total organic carbon (TOC) concentration of CBC400, CBCS, CBCL, SW a-BC, and a-AC (Spearman test for data with 3 points, $p < 0.01$) (Figure S2). When all a-BCs were analyzed together, no significant correlation existed (Pearson or Spearman test, $p > 0.20$). These results determined that the concentration of a-BCs can be used to predict the reaction rate of TCS when considering a single type of a-BC. If different types of a-BCs were evaluated, other properties need to be taken into account for the reaction rate prediction. For that perspective, there was a significant correlation between the pseudo first-order reaction rate constant and a-BC-bound electrons available for donating (Pearson correlation coefficient, $r = 0.64$, $p = 0.01$) (Figure S3). In addition, the 288 h degradation fraction of TCS was also correlated with the a-BC-bound electrons (Pearson correlation coefficient, $r = 0.82$, $p = 0.04$). For a-BC from different sources, a-BC-bound electrons available for donation could be used to predict the reaction rate constant. In terms of the "reactions" between TCS and a-BC-bound electrons, the pseudo second-order rate constant was determined to be 759 $h^{-1}/(mol\ e^-/L)$ based on the regression between the pseudo first-order reaction rate constant and the concentration of a-BC-bound electrons ($p < 0.05$) (Figure S3).

For the samples with CBC400 (soft material-based) and SW (hard wood-based) a-BC where TCS degradation was relatively high among a-BC samples used in this study, the impact of the reduction period for a-BC on the TCS degradation was also assessed (Figure 3). When the a-BC-bound electrons were slightly different for a-BC reduced for 12 and 24 h, the pseudo first-order reaction rate constant was also close for the two sets of samples. As a comparison, the a-BC-bound electrons were substantially lower for the 6 h-reduced a-BC, and the pseudo first-order reaction rate constant was proportionally lower. To achieve the highest potential for degrading TCS, a-BC needs to be reduced for at least 12 h.

Byproduct Analysis. In parallel to the TCS degradation, Cl^- was detected as a degradation byproduct. Upon the degradation of TCS, Cl^- emerged with the fraction of Cl^-/total chlorine (TOTCl$^-$) increasing sharply after 48 h and reaching 54.2 ± 22.4% and 75.3 ± 12.2% at 288 h for samples of CBC400 and SW a-BC, respectively. The total recovery of chlorine by Cl^- and residual TCS gradually decreased and ranged from 73.5 to 82.6% and 85.1 to 90.0% for CBC400 and SW samples during the period of 96−288 h. This relatively high recovery of chlorine by Cl^- and residual TCS suggests that most of TCS were fully dechlorinated with the remaining of TCS degraded to incompletely dechlorinated byproducts.

Furthermore, for the samples of a-CBC400 with the a-BC concentration in stock suspension, other dechlorination byproducts were analyzed based on the LC-TOFMS analysis. Two major byproducts were detected: a dechlorinated phenoxyphenol (m/z of 252.9829, $C_{12}H_8Cl_2O_2$) and a monochlorinated phenoxyphenol (m/z of 219.0222, $C_{12}H_9ClO_2$). These two products were identified by comparing the accurate masses, retention times, and mass spectra with those of the synthesized standards (5-chloro-2-(4-chlorophenoxy) phenol (CCPP) and 5-chloro-2-(phenoxy) phenol) (CPP) (Figures S4−S7). Note that the C−Cl bonds on the dichlorophenoxyl ring of TCS are more susceptible to cleavage than the C−Cl bond on the phenol ring according to the previous study,[74] which is also supported by the observation of the common fragment ion (m/z of 141.9827, $C_6H_3ClO_2$) from these two products that represent the phenol moiety of TCS without dechlorination. Quantification of the CCPP and CPP products based on the standards indicated that their concentrations were low (<0.5 mg/L). Although only with two standards, we also screened other fragments and molecular peaks from possible dechlorination reactions, including the fully dechlorinated product (2-(phenoxy)phenol (PP)), and none of them were detected (Figure S7). The ortho-positioned electron-drawing ether group may make the Cl easier to knock off. The detection of these two byproducts confirmed the dechlorination reaction. However, there may be other reaction pathways and byproducts that can contribute as much as 25% of chlorine in the system and warrant further investigations.

Reaction Pathways and Kinetic Fitting. For the numerical fittings of reaction kinetics, we proposed reactions between TCS and presumable a-BC-based electron donors, i.e., quinoid groups, including semiquinones and hydroquinones (Figure S8 and Table S3). For further investigation of chemical compositions in a-BCs involved in the reduction, mass spectrometry analysis of CBC400 and SW a-BC has detected over 500 peaks. The highest peak intensities were with m/z of 315.087 and 357.151 for CBC400 and SW a-BC, respectively, with multiple possible quinone-based structures (Figures S9 and S10 and Table S4). In addition, EPR signals for the semiquinone radicals ($g = 2.00315$) have been captured for CBC400 bulk samples when this is minor for the CBC200 bulk biochars, which is consistent with the higher electron-accepting capacity of CBC400 a-BC (Figure S11). These analyses indicate that the reductive degradation of TCS by reduced a-BC is likely derived by the quinone groups, the chemical nature of which requires further investigations.

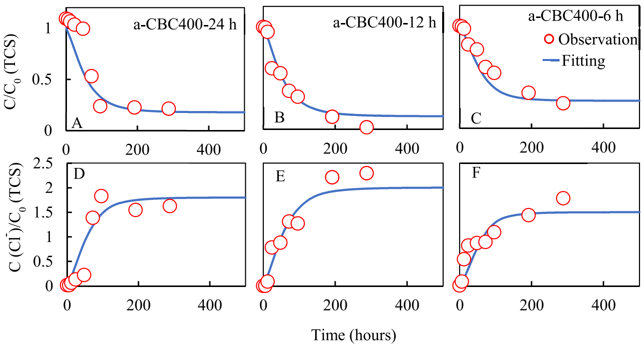

Figure 4. Least squares-based numerical fitting for the kinetics of TCS degradation and generation of Cl^- for the reactions with a-CBC400 pre-reduced for 24 h (A, D), 12 h (B, E), and 6 h (C, F). Circles represent measurement, and the blue lines stand for the fitting results. a-CBC400 represents the aqueous biochar sample prepared using CBC400.

Dechlorination was hypothesized to occur stepwise. Six rate constants for reactions between TCS as well as its degradation byproducts and hydroquinone/semiquinone were fitted using the least-squares method based on the kinetics for TCS degradation and generation of Cl^-. Based on the fitting ($R^2 > 0.76$, Figure 4), the reaction rate constants ranged from 4.48×10^{-5} to 1.65×10^{-2} h^{-1} for the reactions between a-BC and TCS (Figure S12). Consistent with the high recovery of chlorine as Cl^- and residual TCS, the second step and third step dechlorination were faster than the first step. For a-CBC400, consideration of kinetics for additional byproducts can alter the fitting results (Figure S13), but the trend stays in that the first step dechlorination was much slower than the following reactions. In the literature, there are inconsistent reports regarding the relationship between the reaction rate for the different steps of dechlorination.[75−79] Scherer et al.[79] developed the linear free-energy relationships (LFER) for predicting the dechlorination rate for chlorinated aliphatics and found that the rate constant decreased dramatically from trihalogenated aliphatics to dehalogenated aliphatics to monohalogenated aliphatics. Dechlorination of polychlorinated biphenyls was determined to increase with the number of chlorine with the molecules.[76,77] The contrast trend for the reaction rate constant with the chlorination number has also been reported.[75,80] In this study, we found that the first-step dechlorination was much slower than the removal of remaining chlorine for which the full understanding warrants more investigations. The electron attraction of chlorine and its impact on the accessibility of remaining aromatic rings can be an essential regulating factor for the degradation rate.

Environmental Implications. This study has demonstrated a novel dehalogenation reaction between a model organohalogen compound (TCS) by a-BC with an apparent first-order rate constant of 0.0011−0.011 h^{-1}. As a comparison, the reduced aqueous activated carbon can also degrade TCS with a first-order rate constant of 0.0075 h^{-1}. Although the reaction was slower than other abiotic reductive dehalogenation reactions such as by nZVI, the electron transfer between a-BCs and the organohalogen compound is efficient. The advantages of a-BC being environmentally friendly and cost-effective and that these reactions do not produce any byproducts as precipitates make these reactions promising for its potential applications in engineering treatment, including removal of organohalogen from wastewater effluent and remediation of contaminated groundwater. The concentration of a-BC can impact the reaction rate roughly linearly, and it has been demonstrated that a-BC can be mobilized substantially with sonication or other methods. It can enable and further promote the large-scale application of a-BCs in degrading important organohalogen compounds. With the anaerobic dehalogenation by pre-reduced a-BCs demonstrated unambiguously in this study, the direct addition of a-BCs to enhance microbial degradation as electron shuttles would be also feasible.

Although there have been substantial interest in the reactions of biochar materials and their applications in agricultural and engineering systems, to the best of our knowledge, there is rarely a report about the reductive dehalogenation by a-BC. Bulk biochar can sorb the compounds, which can consequently slow down their reactions. Differently, association with a-BC may not alter the availability and reactions of compounds due to the size of a-BC; reduced a-BC can act as a strong electron donor to reductively degrade organohalogen. While, in this study, a common dissimilatory reductive bacteria (*Shewanella*) was used to produce reduced a-BC, other reactions, including the abiotic reactions, can also be used to generate reduced a-BC. Last but not least, TCS was used as a model organohalogen compound in this study. It has been phased out for significant use nationally in the United States. Still, it remains a concern for the quality of water bodies due to its persistence under certain geochemical conditions. The pathways for reactions between TCS and a-BC can shed light on the possible reactions between a-BC and other persistent organohalogens. Our experimental observations and numerical fittings determined that the first step dechlorination was the rate-limiting step for the multi-step dehalogenation reactions. Reactions between a-BC and other organohalogen compounds as well as pathways and the chemical nature of reactive components require further studies.

■ ASSOCIATED CONTENT

Supporting Information

The Supporting Information is available free of charge at https://pubs.acs.org/doi/10.1021/acs.est.0c05940.

> Information on calibration curves for triclosan (Figure S1), correlation between the pseudo first-order rate constant for the degradation of TCS and the organic carbon content and electron donating capacity of the biochars (Figures S2, S3, and S7), byproduct analysis for the degradation of TCS (Figures S4 and S5), kinetics of chloride generation during the degradation (Figure S6), reaction schematics (Figure S8), characterization of bulk and aqueous biochar (Figures S4 and S9−S11 and Table S1), numerical fitting for the reaction kinetics (Figures S12 and S13 and Table S3), and description of the control's setup (Table S2) (PDF)

■ AUTHOR INFORMATION

Corresponding Author

Yu Yang − *Department of Civil and Environmental Engineering, University of Nevada, Reno, Nevada 89557-0258, United States;* orcid.org/0000-0002-7568-0202; Email: yuy@unr.edu

Authors

Srinidhi Lokesh − *Department of Civil and Environmental Engineering, University of Nevada, Reno, Nevada 89557-0258, United States*

Juhee Kim − *School of Civil and Environmental Engineering, Georgia Institute of Technology, Atlanta, Georgia 30332-0355, United States*

Yuwei Zhou − *Department of Civil and Environmental Engineering, University of Nevada, Reno, Nevada 89557-0258, United States*

Danping Wu − *Faculty of Environmental Science and Engineering, Kunming University of Science and Technology, Kunming 650500, China*

Bo Pan − *Faculty of Environmental Science and Engineering, Kunming University of Science and Technology, Kunming 650500, China;* orcid.org/0000-0003-3680-1451

Xilong Wang − *Laboratory for Earth Surface Processes, College of Urban and Environmental Sciences, Peking University, Beijing 100871, P.R. China;* orcid.org/0000-0002-5668-9703

Sebastian Behrens − *Department of Civil, Environmental, and Geo-Engineering, University of Minnesota, Minneapolis, Minnesota 55455-0116, United States*

Ching-Hua Huang − *Department of Civil and Environmental Engineering, University of Nevada, Reno, Nevada 89557-0258, United States;* orcid.org/0000-0002-3786-094X

Complete contact information is available at: https://pubs.acs.org/10.1021/acs.est.0c05940

Notes

The authors declare no competing financial interest.

■ ACKNOWLEDGMENTS

This study was supported by funding from the National Science Foundation (no. NSF 1804209).

■ REFERENCES

(1) Letcher, R. J.; Gebbink, W. A.; Sonne, C.; Born, E. W.; McKinney, M. A.; Dietz, R. Bioaccumulation and Biotransformation of Brominated and Chlorinated Contaminants and Their Metabolites in Ringed Seals (Pusa Hispida) and Polar Bears (Ursus Maritimus) from East Greenland. *Environ. Int.* **2009**, *35*, 1118−1124.

(2) Bhatt, P.; Kumar, M. S.; Mudliar, S.; Chakrabarti, T. Biodegradation of Chlorinated Compounds—A Review. *Crit. Rev. Environ. Sci. Technol.* **2007**, *37*, 165−198.

(3) Redon, P. O.; Abdelouas, A.; Bastviken, D.; Cecchini, S.; Nicolas, M.; Thiry, Y. Chloride and Organic Chlorine in Forest Soils: Storage, Residence Times, And Influence of Ecological Conditions. *Environ. Sci. Technol.* **2011**, *45*, 7202−7208.

(4) Vriens, A.; Nawrot, T. S.; Janssen, B. G.; Baeyens, W.; Bruckers, L.; Covaci, A.; De Craemer, S.; De Henauw, S.; Den Hond, E.; Loots, I.; Nelen, V.; Schettgen, T.; Schoeters, G.; Martens, D. S.; Plusquin, M. Exposure to Environmental Pollutants and Their Association with Biomarkers of Aging: A Multipollutant Approach. *Environ. Sci. Technol.* **2019**, *53*, 5966−5976.

(5) Pessah, I. N.; Lein, P. J.; Seegal, R. F.; Sagiv, S. K. Neurotoxicity of Polychlorinated Biphenyls and Related Organohalogens. *Acta Neuropathol.* **2019**, *138*, 363−387.

(6) Adrian, L.; Löffler, F. E. Organohalide-Respiring Bacteria—An Introduction. In *Organohalide-Respiring Bacteria*; Adrian, L., Löffler, F. E., Eds.; Springer: Berlin, Heidelberg, 2016; pp 3−6, DOI: 10.1007/978-3-662-49875-0_1.

(7) Bellar, T. A.; Lichtenberg, J. J.; Kroner, R. C. The Occurrence of Organohalides in Chlorinated Drinking Waters. *J. - Am. Water Works Assoc.* **1974**, *66*, 703−706.

(8) Häggblom, M. M., Bossert, I. D. Eds. *Dehalogenation: Microbial Processes and Environmental Applications*; Kluwer Academic Publishers: Boston, U.S.A., 2003.

(9) Khan, K. N. M.; Hard, G. C.; Alden, C. L. Chapter 47 - Kidney. In *Haschek and Rousseaux's Handbook of Toxicologic Pathology*; (Third Edition), Haschek, W. M.; Rousseaux, C. G.; Wallig, M. A., Eds.; Academic Press: Boston 2013; pp. 1667−1773, DOI: 10.1016/B978-0-12-415759-0.00047-9.

(10) Kodavanti, P. R. S.; Loganathan, B. Organohalogen Pollutants and Human Health. In *International Encyclopedia of Public Health*; (Second Edition); Quah, S.R.; Cockerham, W.C., Eds.; Oxford: Academic Press, 2017; pp. 359−366, DOI: 10.1016/B978-0-12-803678-5.00318-0.

(11) Vreugdenhil, H. J. I.; Slijper, F. M. E.; Mulder, P. G. H.; Weisglas-Kuperus, N. Effects of Perinatal Exposure to PCBs and Dioxins on Play Behavior in Dutch Children at School Age. *Environ. Health Perspect.* **2002**, *110*, A593−A598.

(12) Richardson, S. D. Disinfection By-Products and Other Emerging Contaminants in Drinking Water. *TrAC Trends Anal. Chem.* **2003**, *22*, 666−684.

(13) Richardson, S. D.; Ternes, T. A. Water Analysis: Emerging Contaminants and Current Issues. *Anal. Chem.* **2018**, *90*, 398−428.

(14) Field, J. A.; Sierra-Alvarez, R. Microbial Transformation and Degradation of Polychlorinated Biphenyls. *Environ. Pollut.* **2008**, *155*, 1−12.

(15) Kookana, R. S.; Ying, G.-G.; Waller, N. J. Triclosan: Its Occurrence, Fate and Effects in the Australian Environment. *Water Sci. Technol.* **2011**, *63*, 598−604.

(16) Liu, J.; Mejia Avendaño, S. Microbial Degradation of Polyfluoroalkyl Chemicals in the Environment: A Review. *Environ. Int.* **2013**, *61*, 98−114.

(17) Singer, H.; Müller, S.; Tixier, C.; Pillonel, L. Triclosan: Occurrence and Fate of a Widely Used Biocide in the Aquatic Environment: Field Measurements in Wastewater Treatment Plants, Surface Waters, and Lake Sediments. *Environ. Sci. Technol.* **2002**, *36*, 4998−5004.

(18) Sinkkonen, S.; Paasivirta, J. Degradation Half-Life Times of PCDDs, PCDFs and PCBs for Environmental Fate Modeling. *Chemosphere* **2000**, *40*, 943−949.

(19) Ying, G. G.; Yu, X. Y.; Kookana, R. S. Biological Degradation of Triclocarban and Triclosan in a Soil under Aerobic and Anaerobic Conditions and Comparison with Environmental Fate Modelling. *Environ. Pollut.* **2007**, *150*, 300−305.

(20) Exner, M.; Färber, H. Perfluorinated Surfactants in Surface and Drinking Waters. *Environ. Sci. Pollut. Res. Int.* **2006**, *13*, 299−307.

(21) Atashgahi, S.; Liebensteiner, M. G.; Janssen, D. B.; Smidt, H.; Stams, A. J. M.; Sipkema, D. Microbial Synthesis and Transformation of Inorganic and Organic Chlorine Compounds. *Front. Microbiol.* **2018**, *9*, 3079.

(22) Nikel, P. I.; Pérez-Pantoja, D.; de Lorenzo, V. Why are chlorinated pollutants so difficult to degrade aerobically? Redox stress limits 1,3-dichloprop-1-ene metabolism by Pseudomonas pavonaceae. *Philos. Trans. R. Soc. London, Ser. B* **2013**, *368*, 20120337.

(23) Berggren, D. R. V.; Marshall, I. P. G.; Azizian, M. F.; Spormann, A. M.; Semprini, L. Effects of Sulfate Reduction on the Bacterial Community and Kinetic Parameters of a Dechlorinating Culture under Chemostat Growth Conditions. *Environ. Sci. Technol.* **2013**, *47*, 1879−1886.

(24) Mohn, W. W.; Tiedje, J. M. Microbial Reductive Dehalogenation. *Microbiol. Rev.* **1992**, *56*, 482−507.

(25) Wiegel, J.; Wu, Q. Microbial Reductive Dehalogenation of Polychlorinated Biphenyls. *FEMS Microbiol. Ecol.* **2000**, *32*, 1−15.

(26) Weatherill, J. J.; Atashgahi, S.; Schneidewind, U.; Krause, S.; Ullah, S.; Cassidy, N.; Rivett, M. O. Natural Attenuation of Chlorinated Ethenes in Hyporheic Zones: A Review of Key Biogeochemical Processes and in-Situ Transformation Potential. *Water Res.* **2018**, *128*, 362−382.

(27) Zhao, S.; Rogers, M. J.; Ding, C.; He, J. Reductive Debromination of Polybrominated Diphenyl Ethers - Microbes Processes and Dehalogenases. *Front. Microbiol.* **2018**, *9*, 1292.

(28) Xie, T.; Reddy, K. R.; Wang, C.; Yargicoglu, E.; Spokas, K. Characteristics and Applications of Biochar for Environmental Remediation: A Review. *Crit. Rev. Environ. Sci. Technol.* **2014**, *45*, 939.

(29) Li, L.; Zou, D.; Xiao, Z.; Zeng, X.; Zhang, L.; Jiang, L.; Wang, A.; Ge, D.; Zhang, G.; Liu, F. Biochar as a Sorbent for Emerging Contaminants Enables Improvements in Waste Management and Sustainable Resource Use. *J. Cleaner Prod.* **2019**, *210*, 1324−1342.

(30) Oliveira, F. R.; Patel, A. K.; Jaisi, D. P.; Adhikari, S.; Lu, H.; Khanal, S. K. Environmental Application of Biochar: Current Status and Perspectives. *Bioresour. Technol.* **2017**, *246*, 110−122.

(31) Kong, L.-L.; Liu, W.-T.; Zhou, Q.-X. Biochar: An Effective Amendment for Remediating Contaminated Soil. *Rev. Environ. Contam. Toxicol.* **2014**, *228*, 83−99.

(32) Cui, L.; Yin, C.; Chen, T.; Quan, G.; Ippolito, J. A.; Liu, B.; Yan, J.; Ding, C.; Hussain, Q.; Umer, M. Remediation of Organic Halogen- Contaminated Wetland Soils Using Biochar. *Sci. Total Environ.* **2019**, *696*, 134087.

(33) Li, Y.; Liu, X.; Wu, X.; Dong, F.; Xu, J.; Pan, X.; Zheng, Y. Effects of Biochars on the Fate of Acetochlor in Soil and on Its Uptake in Maize Seedling. *Environ. Pollut.* **2018**, *241*, 710−719.

(34) Yuan, Y.; Bolan, N.; Prévoteau, A.; Vithanage, M.; Biswas, J. K.; Ok, Y. S.; Wang, H. Applications of Biochar in Redox-Mediated Reactions. *Bioresour. Technol.* **2017**, *246*, 271−281.

(35) Klüpfel, L.; Keiluweit, M.; Kleber, M.; Sander, M. Redox Properties of Plant Biomass-Derived Black Carbon (Biochar). *Environ. Sci. Technol.* **2014**, *48*, 5601−5611.

(36) Lefèvre, E.; Bossa, N.; Gardner, C. M.; Gehrke, G. E.; Cooper, E. M.; Stapleton, H. M.; Hsu-Kim, H.; Gunsch, C. K. Biochar and Activated Carbon Act as Promising Amendments for Promoting the Microbial Debromination of Tetrabromobisphenol A. *Water Res.* **2018**, *128*, 102−110.

(37) Yu, L.; Yuan, Y.; Tang, J.; Wang, Y.; Zhou, S. Biochar as an Electron Shuttle for Reductive Dechlorination of Pentachlorophenol by Geobacter Sulfurreducens. *Sci. Rep.* **2015**, *5*, 16221.

(38) Marchal, G.; Smith, K. E. C.; Rein, A.; Winding, A.; de Jonge, L. W.; Trapp, S.; Karlson, U. G. Impact of Activated Carbon, Biochar and Compost on the Desorption and Mineralization of Phenanthrene in Soil. *Environ. Pollut.* **2013**, *181*, 200−210.

(39) Cornelissen, G.; Gustafsson, O.; Bucheli, T. D.; Jonker, M. T. O.; Koelmans, A. A.; Van Noort, P. C. M. Extensive Sorption of Organic Compounds to Black Carbon, Coal, and Kerogen in Sediments and Soils: Mechanisms and Consequences for Distribution, Bioaccumulation, and Biodegradation. *Environ. Sci. Technol.* **2005**, *39*, 6881−6895.

(40) Yang, Y.; Hunter, W.; Tao, S.; Crowley, D.; Gan, J. Effect of Activated Carbon on Microbial Bioavailability of Phenanthrene in Soils. *Environ. Toxicol. Chem.* **2009**, *28*, 2283−2288.

(41) Koelmans, A. A.; Jonker, M. T. O.; Cornelissen, G.; Bucheli, T. D.; Van Noort, P. C. M.; Gustafsson, Ö. Black Carbon: The Reverse of Its Dark Side. *Chemosphere* **2006**, *63*, 365−377.

(42) Liu, G.; Zheng, H.; Jiang, Z.; Zhao, J.; Wang, Z.; Pan, B.; Xing, B. Formation and Physicochemical Characteristics of Nano Biochar: Insight into Chemical and Colloidal Stability. *Environ. Sci. Technol.* **2018**, *52*, 10369−10379.

(43) Song, B.; Chen, M.; Zhao, L.; Qiu, H.; Cao, X. Physicochemical Property and Colloidal Stability of Micron- and Nano-Particle Biochar Derived from a Variety of Feedstock Sources. *Sci. Total Environ.* **2019**, *661*, 685−695.

(44) Kux, L. *Federal Register*; Authenticated U.S. Government Information; 2016, Vol. 81 No. 126.

(45) Weatherly, L. M.; Gosse, J. A. Triclosan Exposure, Transformation, and Human Health Effects. *J. Toxicol. Environ. Health, B* **2017**, *20*, 447−469.

(46) Casey, Schmidt *Assessment of Pinyon and Juniper Derived Biochar as a Soil Amendment to Increase Survival of Urban Trees in Nevada*; Division of life sciences: Desert Research Institute: 2013.

(47) Yanala, S. R. Use of Biochar to Produce Reclaimed Water for Irrigation Reuse Purposes. ProQuest Dissertations Publishing, 2019.

(48) Roden, E. E.; Kappler, A.; Bauer, I.; Jiang, J.; Paul, A.; Stoesser, R.; Konishi, H.; Xu, H. Extracellular Electron Transfer through Microbial Reduction of Solid-Phase Humic Substances. *Nat. Geosci.* **2010**, *3*, 417−421.

(49) Xu, S.; Adhikari, D.; Huang, R.; Zhang, H.; Tang, Y.; Roden, E.; Yang, Y. Biochar-Facilitated Microbial Reduction of Hematite. *Environ. Sci. Technol.* **2016**, *50*, 2389−2395.

(50) Zall, D. M.; Fisher, D.; Garner, M. Q. Photometric Determination of Chlorides in Water. *Anal. Chem* **1956**, *28*, 1665−1668.

(51) Hamilton, R. H. A Direct Photometric Method for Chloride in Biological Fluids, Employing Mercuric Thiocyanate and Perchloric Acid. *Clin. Chem.* **1966**, *12*, 1−17.

(52) Rajapaksha, A. U.; Ok, Y. S.; El-Naggar, A.; Kim, H.; Song, F.; Kang, S.; Tsang, Y. F. Dissolved Organic Matter Characterization of Biochars Produced from Different Feedstock Materials. *J. Environ. Manage.* **2019**, *233*, 393−399.

(53) Yang, W.; Shang, J.; Sharma, P.; Li, B.; Liu, K.; Flury, M. Colloidal Stability and Aggregation Kinetics of Biochar Colloids: Effects of Pyrolysis Temperature, Cation Type, and Humic Acid Concentrations. *Sci. Total Environ.* **2019**, *658*, 1306−1315.

(54) Keiluweit, M.; Nico, P. S.; Johnson, M. G.; Kleber, M. Dynamic Molecular Structure of Plant Biomass-Derived Black Carbon (Biochar). *Environ. Sci. Technol.* **2010**, *44*, 1247−1253.

(55) Heymann, K.; Lehmann, J.; Solomon, D.; Schmidt, M. W. I.; Regier, T. C 1s K-Edge near Edge X-Ray Absorption Fine Structure (NEXAFS) Spectroscopy for Characterizing Functional Group Chemistry of Black Carbon. *Org. Geochem.* **2011**, *42*, 1055−1064.

(56) Jiang, S.; Nguyen, T. A. H.; Rudolph, V.; Yang, H.; Zhang, D.; Ok, Y. S.; Huang, L. Characterization of Hard- and Softwood Biochars Pyrolyzed at High Temperature. *Environ. Geochem. Health* **2017**, *39*, 403−415.

(57) Tomczyk, A.; Sokołowska, Z.; Boguta, P. Biochar Physicochemical Properties: Pyrolysis Temperature and Feedstock Kind Effects. *Rev. Environ. Sci. Bio/Technol.* **2020**, *19*, 191−215.

(58) Lehmann, J. Bio-Energy in the Black. *Front. Ecol. Environ.* **2007**, *preprint*, 381−387.

(59) Pariyar, P.; Kumari, K.; Jain, M. K.; Jadhao, P. S. Evaluation of Change in Biochar Properties Derived from Different Feedstock and Pyrolysis Temperature for Environmental and Agricultural Application. *Sci. Total Environ.* **2020**, *713*, 136433.

(60) Van der Zee, F. P.; Bisschops, I. A. E.; Lettinga, G.; Field, J. A. Activated Carbon as an Electron Acceptor and Redox Mediator during the Anaerobic Biotransformation of Azo Dyes. *Environ. Sci. Technol.* **2003**, *37*, 402−408.

(61) Wang, Z.; Liu, C.; Wang, X.; Marshall, M. J.; Zachara, J. M.; Rosso, K. M.; Dupuis, M.; Fredrickson, J. K.; Heald, S.; Shi, L. Kinetics of Reduction of Fe(III) Complexes by Outer Membrane Cytochromes MtrC and OmcA of Shewanella Oneidensis MR-1. *Appl. Environ. Microbiol.* **2008**, *74*, 6746−6755.

(62) Curtis, G. P.; Reinhard, M. Reductive Dehalogenation of Hexachlorethane. Carbon- Tetrachloride, and Bromoform by Anthrahydroquinone Disulfonate and Humic- Acid. *Environ. Sci. Technol.* **1994**, *28*, 2393−2401.

(63) Keum, Y. S.; Li, Q. X. Reductive Debromination of Polybrominated Diphenyl Ethers by Zerovalent Iron. *Environ. Sci. Technol.* **2005**, *39*, 2280−2286.

(64) Martínez, C. M.; Alvarez, L. H.; Cervantes, F. J. Simultaneous Biodegradation of Phenol and Carbon Tetrachloride Mediated by Humic Acids. *Biodegradation* **2012**, *23*, 635−644.

(65) Wang, Y.; Wu, C.; Wang, X.; Zhou, S. The Role of Humic Substances in the Anaerobic Reductive Dechlorination of 2,4-Dichlorophenoxyacetic Acid by Comamonas Koreensis Strain CY01. *J. Hazard. Mater.* **2009**, *164*, 941−947.

(66) Chan, K.-Y.; Xu, L.-C.; Fang, H. H. P. Anaerobic Electrochemical Corrosion Rug of Mild Steel in the Presence of Extracellular Polymeric Substances Produced by a Culture Enriched in Sulfate-Reducing Bacteria. *Environ. Sci. Technol.* **2002**, *36*, 1720−1727.

(67) Bokare, V.; Murugesan, K.; Kim, Y. M.; Jeon, J. R.; Kim, E. J.; Chang, Y. S. Degradation of triclosan by an integrated nano-bio redox process. *Bioresour. Technol.* **2010**, *101*, 6354−6360.

(68) Zhuang, Y.; Ahn, S.; Luthy, R. G. Debromination of Polybrominated Diphenyl Ethers by Nanoscale Zerovalent Iron: Pathways, Kinetics, and Reactivity. *Environ. Sci. Technol.* **2010**, *44*, 8236−8242.

(69) Trainer, E. L.; Ginder-Vogel, M.; Remucal, C. K. Organic Structure and Solid Characteristics Determine Reactivity of Phenolic Compounds with Synthetic and Reclaimed Manganese Oxides. *Environ. Sci.: Water Res. Technol.* **2020**, *6*, 540−553.

(70) Fu, H.; Guo, Y.; Chen, W.; Gu, C.; Zhu, D. Reductive Dechlorination of Hexachloroethane by Sulfide in Aqueous Solutions Mediated by Graphene Oxide and Carbon Nanotubes. *Carbon* **2014**, *72*, 74−81.

(71) Toral-Sánchez, E.; Rangel-Mendez, J. R.; Hurt, R. H.; Valdés, J. A. A.; Aguilar, C. N.; Cervantes, F. J. Novel Application of Magnetic Nano-Carbon Composite as Redox Mediator in the Reductive Biodegradation of Iopromide in Anaerobic Continuous Systems. *Appl. Microbiol. Biotechnol.* **2018**, *102*, 8951−8961.

(72) Gavaskar, A.; Tatar, L.; Condit, W. *Nanoscale Zero-Valent Iron Technologies for Source Remediation. Cost and performance report*; Naval Facilities Engineering Command: Columbus, Ohio, USA, 2005.

(73) Jirka, S.; Tomlinson, T. *State of the Biochar Industry; Survey*; International Biochar Initiative: New York, USA, 2014 2013.

(74) Kliegman, S.; Eustis, S. N.; Arnold, W. A.; McNeill, K. Experimental and Theoretical Insights into the Involvement of Radicals in Triclosan Phototransformation. *Environ. Sci. Technol.* **2013**, *47*, 6756−6763.

(75) Arnold, W. A.; Roberts, A. L. Pathways and Kinetics of Chlorinated Ethylene and Chlorinated Acetylene Reaction with Fe(0) Particles. *Environ. Sci. Technol.* **2000**, *34*, 1794−1805.

(76) Kim, J.-H.; Tratnyek, P. G.; Chang, Y.-S. Rapid Dechlorination of Polychlorinated Dibenzo-p-Dioxins by Bimetallic and Nanosized Zerovalent Iron. *Environ. Sci. Technol.* **2008**, *42*, 4106−4112.

(77) Lowry, G. V.; Johnson, K. M. Congener-Specific Dechlorination of Dissolved PCBs by Microscale and Nanoscale Zerovalent Iron in a Water/Methanol Solution. *Environ. Sci. Technol.* **2004**, *38*, 5208−5216.

(78) Wang, C.-B.; Zhang, W. Synthesizing Nanoscale Iron Particles for Rapid and Complete Dechlorination of TCE and PCBs. *Environ. Sci. Technol.* **1997**, *31*, 2154−2156.

(79) Scherer, M. M.; Balko, B. A.; Gallagher, D. A.; Tratnyek, P. G. Correlation Analysis of Rate Constants for Dechlorination by Zero-Valent Iron. *Environ. Sci. Technol.* **1998**, *32*, 3026−3033.

(80) Butler, E. C.; Hayes, K. F. Kinetics of the Transformation of Trichloroethylene and Tetrachloroethylene by Iron Sulfide. *Environ. Sci. Technol.* **1999**, *33*, 2021−2027.